

# Cu<sub>x</sub>O Nanostructure-Based Gas Sensors

Subjects: [Engineering](#), [Chemical](#)

Contributor: Ali Mirzaei

H<sub>2</sub>S gas is a toxic and hazardous byproduct of the oil and gas industries. It paralyzes the olfactory nerves, with concentrations above 100 ppm, resulting in loss of smell; prolonged inhalation may even cause death. One of the most important semiconducting metal oxides for the detection of H<sub>2</sub>S is Cu<sub>x</sub>O (x = 1, 2), which is converted to Cu<sub>x</sub>S upon exposure to H<sub>2</sub>S, leading to a remarkable modulation in the resistance and appearance of an electrical sensing signal.

gas sensor

HS gas

CuO

CuS

sensing mechanism

## 1. Overview of H<sub>2</sub>S Gas Properties

H<sub>2</sub>S, which has a disagreeable odor, is a colorless, highly toxic, corrosive, flammable, and explosive gas [\[1\]\[2\]](#). It has various sources, including volcanic eruptions, anaerobic decay of organic materials, Kraft paper mills, processing of gasoline, natural gas, coal, and sewage, as well as petroleum refining [\[3\]\[4\]\[5\]\[6\]](#). Other sources of H<sub>2</sub>S include decomposition of fish in the fishing industry and waste biodegradation in shrimp farms [\[7\]](#). H<sub>2</sub>S is readily oxidized by atmospheric oxygen when irradiated with sunlight and can form SO<sub>2</sub> and H<sub>2</sub>SO<sub>4</sub> in the atmosphere, leading to acid rains [\[8\]](#). Moreover, because H<sub>2</sub>S is heavier than air, it remains in the atmosphere for up to 18 h; thus, it can easily accumulate in areas such as mine tunnels, sewers, and manure tanks [\[9\]\[10\]](#). As stated by the *United States Occupational Safety and Health Administration* (US-OSHA, Washington, DC, USA), the concentration limit for exposure to H<sub>2</sub>S within 8 h is approximately 20 ppm [\[11\]](#). Exposure to low levels of H<sub>2</sub>S may result in eye and throat injuries, dizziness, memory impairment, and loss of reasoning and balance [\[12\]\[13\]\[14\]\[15\]](#). Continuous exposure to H<sub>2</sub>S at 2 ppm causes nausea/headaches, while 20 ppm results in fatigue and headache, and concentrations of 50–100 ppm result in loss of appetite, respiratory tract irritation, digestion issues, and loss of breathing with high possibility of death [\[13\]\[16\]](#). Moreover, an individual's olfaction may quickly fail to function properly when exposed to H<sub>2</sub>S levels of more than 100 ppm for a short period of time [\[17\]](#). Prolonged exposure to 100 ppb of H<sub>2</sub>S also affects respiration in human cells and causes a deficiency of oxygen in systemic tissues, endangering human health [\[18\]\[19\]](#). H<sub>2</sub>S exposure at concentrations of 1000 ppm and above would result in immediate death. For example, 21 fatalities were reported in the Gulf of Mexico in 2007 as a result of H<sub>2</sub>S leaks and chain accidents on the Kab-121 platform [\[20\]](#). In addition, H<sub>2</sub>S is a known biomarker for various diseases such as Down syndrome, Alzheimer's disease, ischemia, asthma, and halitosis [\[21\]](#). For example, the H<sub>2</sub>S concentration (~100–500 ppb) in the breath of patients with halitosis is greater than that in healthy individuals. This is primarily due to local oral diseases and certain systemic diseases, such as digestive issues [\[22\]](#). Accordingly, detection of H<sub>2</sub>S gas is important from the perspectives of safety, industry, and medicine.

## 2. Motivation for the Use of Cu<sub>x</sub>O as a H<sub>2</sub>S Gas Sensor

To date, several types of gas sensors, including chemoresistive gas sensors made of semiconducting metal oxides, electrochemical sensors, optical sensors, and piezoelectric sensors, have been utilized for H<sub>2</sub>S gas detection [23][24][25]. Among them, semiconducting metal oxide gas sensors are widely popular owing to their advantages such as simple operation, small size, low cost, high sensitivity, high stability, fast response, and long life [26][27]. Overall, the sensing mechanism in this type of gas sensor is the change in resistance caused by exposure to target gases [28][29]. The gas response depends mainly on the contact between the target gases and the surface of the sensing element, as well as the adsorption sites on the sensor surface [30]. Among the different metal oxides used for H<sub>2</sub>S-sensing, Cu<sub>x</sub>O (x = 1, 2) is an exception. CuO is a low-cost semiconducting metal oxide (energy gap = 1.2 eV) and has a monoclinic crystal structure [31]. It can directly react with H<sub>2</sub>S to form a Cu<sub>x</sub>S layer with high conductivity. Primarily, CuS forms clusters on the surface of CuO, which grows progressively and links to create a persistent CuS phase with metallic-like conductivity. This process generates a conductive percolation pathway, which consequently decreases the resistance abruptly [32]. The electrons flow from CuO to CuS owing to the difference in their work functions and formation of a potential barrier. When the grain boundaries transform into CuS, the width of the potential barrier is minimized, and the conductivity changes from semiconducting to metallic, resulting in an advanced H<sub>2</sub>S response [33]. Thus, Cu<sub>x</sub>O is highly popular for H<sub>2</sub>S gas-sensing studies [12][26][34]. Furthermore, it can be used as an adsorbent for the purification of gas streams, especially by H<sub>2</sub>S removal [35]. In addition, the selectivity of Cu<sub>x</sub>O can be related to the lower bond energy of H<sub>2</sub>S relative to other gases. As shown in Table 1, the H–SH bonding energy in H<sub>2</sub>S is 381 kJ/mol, which is lower than that of most interfering gases, leading to better interaction and dissociation of the surface of the sensing material.

**Table 1.** Various gas molecules and their properties [36].

Gas	Ammonia (NH <sub>3</sub> )	Hydrogen (H <sub>2</sub> )	Methane (CH <sub>4</sub> )	Carbon Monoxide (CO)	H <sub>2</sub> S
Bond	H–NH <sub>2</sub>	H–H	H–CH <sub>3</sub>	C–O	H–SH
Bond Energy (kJ/mol)	435	436	431	1076	381
Molecular Size (nm)	0.26	0.289	0.38	0.37	0.34

## 3. Gas Sensors Based on Pristine Cu<sub>x</sub>O Nanostructures

Hu et al. [37] conducted a study on the magnetron sputtering of p-type CuO nanoneedle arrays followed by wet chemical etching and annealing. Their CuO sensor demonstrated response of 76.5% ( $\Delta R/R_a$ ) × 100 to 15 ppm H<sub>2</sub>S gas at 150 °C. The oxygen molecules from air are adsorbed onto the sensor surface to form a hole accumulation layer (HAL); thereafter, the sensor resistance decreases relative to vacuum because of the adsorption of electrons as follows [37]:



When the sensor is in an H<sub>2</sub>S atmosphere, the chemical reaction between the adsorbed H<sub>2</sub>S molecules on the sensor surface and the chemisorbed oxygen species occurs as follows:



The released electrons are combined with holes, and the thickness of the HAL decreases. Thus, the resistance increases, which leads to the appearance of a sensing signal. However, the authors did not report the formation of CuS, and the selectivity of the gas sensor was not explained. In another study, Huang et al. synthesized sea anemone-like CuO nanoarrays in situ via a seed-induced hydrothermal method at different time durations (1–6 h) [38]. For growth times exceeding 2 h, they observed that the CuO nanostructures grew among the electrodes, and CuO nanostructures and sea anemone array morphologies were formed. The surface areas of CuO nanoarrays prepared for 2, 3, 4, 5, and 6 h were 5.85, 7.35, 7.03, 6.67, and 5.70 m<sup>2</sup>·g<sup>-1</sup>, respectively. The surface area decreased with increasing growth time (>2 h). The results of H<sub>2</sub>S gas-sensing showed that the CuO prepared for 2 h had the lowest response among the other sensors because of the fragile continuity of the tiny CuO nanoarrays, which did not offer the active electrical conduction pathways necessary for the H<sub>2</sub>S-sensing reactions. The sensor with the largest surface area (prepared for 3 h) showed not only the highest response to H<sub>2</sub>S gas (24.08 to 5 ppb H<sub>2</sub>S gas at 25 °C), but also good selectivity.

The HAL was formed in air, and the oxygen adsorption made it wider at the junctions, which enabled hole transmission and subsequently decreased the resistance. In the H<sub>2</sub>S gas atmosphere, the HAL was narrowed, which hampered the transmission of holes while the sensor resistance increased. In addition, the cross-linked assembly enabled the adsorption, dispersion, and channeling of H<sub>2</sub>S molecules in detecting reactions and efficiently evaded the lateral stacking and accumulation of CuO nanostructures with no specific surface area loss because of the slight contact and appropriate clearance. This eventually led to a high sensitivity of the gas sensor toward H<sub>2</sub>S gas.

As humidity is always present in real environments, the development of gas sensors that can operate under humid conditions is important. Accordingly, Miao et al. [39] described the humidity-independent H<sub>2</sub>S-sensing performance of hydrothermally processed monolayered CuO nanosheet films under dry and wet conditions. [Figure 1](#)a,b compares the sensing mechanism of the CuO gas sensor to H<sub>2</sub>S in dry and humid environments. In particular, in the humid state, previously adsorbed oxygen anions are substituted partly via terminal hydroxyl groups, which results in low reactions between H<sub>2</sub>S molecules and chemisorbed oxygen atoms. The extent of this limit was determined on the basis of the humidity level in the gas chamber. Accordingly, the sensor signal to H<sub>2</sub>S decreased steadily as the humidity level increased. However, in H<sub>2</sub>S-sensing, the inclusion of S in the CuO framework was assisted by the terminal hydroxyl group at the surface. In addition, the higher humidity level resulted in an

abundance of terminal hydroxyl groups, and, as a result, greater conversion from CuO to Cu<sub>2</sub>S and S occurred. This was due to variable oxidation states of Cu and was demonstrated by XPS and SEM studies. Thus, the sensor response was maintained at the same level as the humidity increased. The decreased recovery time observed under humid conditions was elucidated through the low thermal stability of Cu<sub>2</sub>S. The characteristic Gibbs free energies for the development for CuO, Cu<sub>2</sub>O, and Cu<sub>2</sub>S were -129.7 kJ/mol, -146.0 kJ/mol, and -86.2 kJ/mol, respectively. In this way, changing from a less thermodynamically steady phase (i.e., Cu<sub>2</sub>S) into CuO would be a much more straightforward process than from a steady phase (Cu<sub>2</sub>O); accordingly, a quicker recovery time was observed under humid conditions [39].

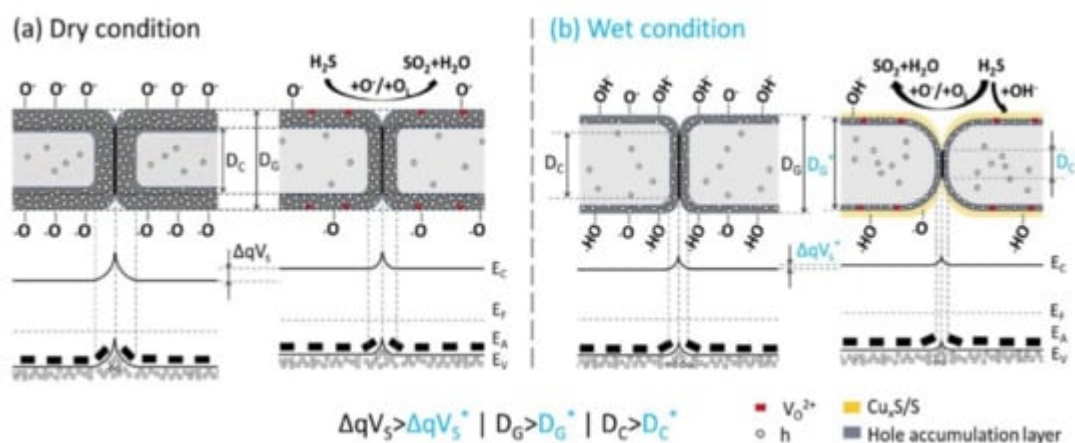


**Figure 1.** Schematic of H<sub>2</sub>S detecting mechanism of p-CuO nanosheet gas sensor in (a) dry and (b) humid environments. Reprinted from [39] with permission from Elsevier.

Dhakshinamoorthy et al. [40] described the H<sub>2</sub>S gas-sensing features of CuO nanocuboids. The fabricated CuO nanocuboid sensor had a response of 2.5 ( $\Delta R/R_a$ ) to 10 ppm H<sub>2</sub>S at an optimal temperature of 200 °C. When H<sub>2</sub>S molecules are adsorbed onto the CuO (111) plane, the 'S' atom can be bonded to two-fold subsurface Cu atom (Cu<sub>sub</sub>) atoms through the bridge bond. However, the 'H' adsorbs favorably on the outermost oxygen (O<sub>surf</sub>) site of the CuO lattice and displays good catalytic activity toward H<sub>2</sub>S dissociation. A comparison of the H<sub>2</sub>S gas-sensing performance of the pristine Cu<sub>x</sub>O gas sensors is shown in Table 2. Different morphologies have been used for H<sub>2</sub>S-sensing at different temperatures. However, pristine Cu<sub>x</sub>O gas sensors show lower sensitivity compared to noble metal-decorated gas sensors or composite gas sensors. Therefore, strategies are needed to enhance the response of gas sensors toward H<sub>2</sub>S gas.

**Table 2.** H<sub>2</sub>S gas-sensing properties of pristine Cu<sub>x</sub>O-based gas sensors.

Sensor	H <sub>2</sub> S Conc. (ppm)	Response (R <sub>g</sub> /R <sub>a</sub> )	LOD † (ppm)	Res. Time (s)/ Rec. Time (s)	T (°C)	Ref.
CuO nanoparticles	5	4.9 ± 0.43	0.2	297.5 ± 9.2/54 ± 7.1	40	[12]

Sensor	H <sub>2</sub> S Conc. (ppm)	Response (R <sub>g</sub> /R <sub>a</sub> )	LOD † (ppb)	Res. Time (s)/ Rec. Time (s)	T (°C)	Ref.
CuO nanoneedles	10	76.5% ( $\Delta R/R_a$ ) × 100	161 ppb	92/196	150	[37]
Sea anemone-like CuO nanoarrays	5 ppb	24.08	1.52 ppb	102/539	25	[38]
CuO nanosheets	400 ppb	1.7	3 ppb	NA *	325	[39]
CuO nanocuboids	10	~2.4 ( $\Delta R/R_a$ )	1	NA	200	[40]
CuO nanosheets	1	325% [ $(\Delta R/R_a) \times 100$ ]	2 ppb	4/9	240	[41]
CuO nanowires	100 ppb	~0.2 ( $\Delta R/R_a$ )	2.5 ppb	10 min/15 min	180	[42]

\* NA: not available; † LOD: limit of detection; T = operating temperature

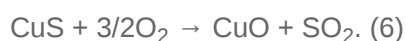
## 4. Pd-Decorated/Doped Cu<sub>x</sub>O Nanostructure-Based Gas Sensors

To boost the sensing performance of metal oxide gas sensors, the addition of noble metals such as Pd, Pt, and Au has been studied extensively because of their electronic and chemical sensitization properties [43][44][45][46][47]. Unfortunately, there are very few studies related to the noble metal decoration on the surface of Cu<sub>x</sub>O nanostructures, and these are discussed below. Kim et al. [27] improved the H<sub>2</sub>S-sensing performance of CuO nanowires (NWs) in self-heating mode through Pd decoration. They used a thermal oxidation method to grow network-like CuO NWs on a patterned interdigital electrode on a SiO<sub>2</sub>-grown Si substrate, and subsequent Pd decoration was achieved through UV irradiation. Their sensing results corroborate that the sensor made of pristine CuO NWs did not show H<sub>2</sub>S selectivity at an optimum temperature of 300 °C. However, the Pd-functionalized CuO NW sensor exhibited a higher response to H<sub>2</sub>S at 100 °C. In addition, the pristine and Pd-loaded sensors showed responses (R<sub>g</sub>/R<sub>a</sub>) of 1.08 and 1.89, respectively, to 100 ppm H<sub>2</sub>S in the self-heating mode at 5 V. The generated heat was due to the self-heating effects attributable to (i) the electron current passing through the CuO NWs, and (ii) the number of networked and directly connected CuO NWs. Because of chemical sensitization, Pd may simply dissociate and transfer oxygen molecules and target gases via the spillover effect. Consequently, higher quantities of gas molecules can reach the surface of the sensor, and, accordingly, a better response is expected. In addition, some Pd can be partially converted into PdO in the air. The electrons flow from CuO to Pd/PdO because of the smaller work function of CuO compared to Pd and PdO. Therefore, an HAL is formed on the CuO side. Upon reducing the gas exposure, the width of the HAL in CuO is condensed. As the initial volume/concentration of holes increases due to the presence of Pd/PdO, the reduction in the same number of holes due to exposure to the reducing gas results in a low response of the sensor. This results in a decrease in the sensor response to the reducing gases. However, the situation is different for H<sub>2</sub>S-sensing. CuO is transformed into CuS with metal-like

conductivity upon exposure to H<sub>2</sub>S, which results in a high resistance modulation at the heterojunctions. The height of the potential barriers decreases owing to the different work functions of CuO and CuS. This results in a higher concentration of electrons in the sensing layer (CuO/CuS) than in CuO, which decreases the concentration of holes and increases the resistance of the sensing material. In the p-type sensor, a smaller conduction volume of the hole region delivers a high sensor response.

In another study, Kim et al. [48] described the development of CuO nanorods (NRs) and their respective Pd-functionalization via a three-step approach including Cu foil oxidation in air, dipping in PdCl<sub>2</sub>, and subsequent annealing. In air, the CuO surface adsorbs oxygen from air by capturing electrons, resulting in the formation of HAL. Upon exposure to low concentrations of H<sub>2</sub>S, the surface reactions occur spontaneously between the formerly adsorbed oxygen species and H<sub>2</sub>S molecules; subsequently, the electrons released from the surface states recombine with the holes in the valence band, leading to an increase in the electrical resistance of the gas sensor. In contrast, at high H<sub>2</sub>S concentrations, a layer of CuS is created on the CuO NR surface. The configuration of CuS reduces the resistance to its metallic character. In the case of Pd/CuO NRs, the adsorption and generation of free electrons through H<sub>2</sub>S gas are advanced on the surface of Pd nanoparticles (NPs). The Pd-NPs have a larger surface area than the CuO NRs, leading to better H<sub>2</sub>S adsorption. The H<sub>2</sub>S molecules dissociate on the catalytic Pd-clusters and diffuse, possibly across and/or through the clusters, to the substrate, wherein H<sub>2</sub>S gas molecules may correlate with the CuO NRs to enhance the resistance. Therefore, through Pd loading, a higher response was observed.

Mikami et al. [49], reported the synthesis of Pd-loaded Cu<sub>2</sub>O nanocrystals, which corroborated the H<sub>2</sub>S responses at low concentrations (1–8 ppm) between 50 °C and 150 °C. The electrical resistance of Cu<sub>2</sub>O was found to increase upon Pd loading because of the configuration of the Schottky junctions between Cu<sub>2</sub>O and Pd. They noticed that the resistance of the sensor decreased abruptly for high Pd loading (5 mol.% and 10 mol.%), signifying that adding a suitable quantity of Pd to the Cu<sub>2</sub>O nanocrystals suppresses Cu<sub>2</sub>O sulfurization and supports the reaction of the adsorbed oxygen with H<sub>2</sub>S. In fact, catalytic H<sub>2</sub>S dissociation on Pd facilitated the reaction of adsorbed oxygen with H<sub>2</sub>S gas. Upon stoppage of H<sub>2</sub>S gas, Cu<sub>2</sub>O and CuO oxides were formed in the air according to the following equations:



The standard Gibbs free energies of Equations (5) and (6) at 50 °C and 150 °C are –359.411, –372.825, –350.166, and –364.33 kJ/mol, respectively, indicating that these reactions are thermodynamically favorable at 50 and 150 °C. This demonstrates the reversible nature of gas sensors.

Lastly, Hu et al. [50] developed a Pd-doped (0–1.5 wt.%) CuO gas sensor for H<sub>2</sub>S-sensing. The ionic radius of Cu<sup>2+</sup> (0.73 Å) is smaller than that of Pd<sup>2+</sup> (0.86 Å), and the replacement of Cu<sup>2+</sup> through Pd<sup>2+</sup> ions induced lattice growth, which was supported by the XRD pattern. Sensing studies showed that the H<sub>2</sub>S response of the Pd-doped CuO (1.25 wt.%) sensor was 7.9 times greater than that of the pristine CuO sensor ( $R_0/R_a = 15.7$ ) at 80 °C. The

upgraded response characteristics of the Pd-doped CuO were largely ascribed to electronic sensitization. Even at room temperature, PdO has a high intrinsic carrier concentration and conductivity; thus, Pd doping can decrease the working temperature of the Pd/CuO sensor. Additionally, PdO is capable of boosting the sensing material to capture oxygen molecules and form chemisorbed oxygen atoms. In addition, due to the sensitization, PdO molecules on the surface of CuO can take part in the reactions and release electrons once they are exposed to H<sub>2</sub>S. Accordingly, the released electrons can be recombined with holes, resulting in a reduction in the concentration of holes. Thereafter, the resistance of the Pd-doped CuO sensor increased with contact with H<sub>2</sub>S. Compared to pristine CuO, Pd-doped CuO (1.25 wt.%) had a superior surface area and high density of adsorption sites, which resulted in excellent responses even at comparatively low H<sub>2</sub>S concentrations. However, surface disorder occurred as the doping concentration increased to 1.50 wt.%, and it was accompanied by an increase in the density of surface states, leading to the pinning of Fermi level surfaces and, hence, a decrease in the sensor response. A list of noble-metal-decorated/doped CuO-based gas sensors for H<sub>2</sub>S detection is presented in [Table 3](#). As can be seen, only Pd has been used in combination with Cu<sub>x</sub>O; in this regard, decoration/doping with other noble metals is essential. In general, Pd-decoration/doping on CuO can enhance the response of gas sensors relative to pristine gas sensors. Furthermore, it can decrease the sensing temperature and increase the stability of gas sensors [\[27\]](#)[\[48\]](#)[\[49\]](#)[\[50\]](#).

**Table 3.** H<sub>2</sub>S gas-sensing properties of noble metal-decorated/doped CuO-based gas sensors.

Sensing Materials	H <sub>2</sub> S Conc. (ppm)	Response (R <sub>g</sub> /R <sub>a</sub> )	LOD (ppm)	Res. Time (s)/ Rec. Time (s)	T (°C)	Ref.
Pd-decorated CuO NWs	100	1.962	1	NA	100	<a href="#">[27]</a>
Pd-decorated CuO nanorods	100	$31,243\%(\Delta R/R_a) \times 100$	20	670/80	300	<a href="#">[48]</a>
Pd (1 mol.%) -loaded CuO nanocrystals	8	7.9	1	NA	250	<a href="#">[49]</a>
Pd-doped CuO nanoflowers	50	123.4	0.1	15/3500	80	<a href="#">[50]</a>

## References

- Hu, Y.; Li, L.; Zhang, L.; Lv, Y. Dielectric barrier discharge plasma-assisted fabrication of g-C<sub>3</sub>N<sub>4</sub>-Mn<sub>3</sub>O<sub>4</sub> composite for high-performance cataluminescence H<sub>2</sub>S gas sensor. *Sens. Actuators B Chem.* 2017, 239, 1177–1184.
- Li, H.; Liu, T.; Su, S.; Jin, M.; Fang, W.; Liu, L.; Wang, Y.; Hu, S.; Xiang, J. Effect of Ce modification on desulfurization performance of regenerated sorbent for high temperature H<sub>2</sub>S removal from coal gas. *Fuel* 2021, 293, 120463.

3. Abdel Rahman, N.S.; Greish, Y.E.; Mahmoud, S.T.; Qamhieh, N.N.; El-Maghraby, H.F.; Zeze, D. Fabrication and characterization of cellulose acetate-based nanofibers and nanofilms for H<sub>2</sub>S gas sensing application. *Carbohydr. Polym.* 2021, 258, 117643.
4. Mirzaei, A.; Kim, S.S.; Kim, H.W. Resistance-based H<sub>2</sub>S gas sensors using metal oxide nanostructures: A review of recent advances. *J. Hazard. Mater.* 2018, 357, 314–331.
5. Zheng, D.; Jiang, Z.; Shi, J.; Wang, Y.; Liu, Z. Experimental analysis of the effect of nitrogen gas on the H<sub>2</sub>S stripping process during the pigging operation of a long crude oil pipeline. *Case Stud. Therm. Eng.* 2020, 22, 100741.
6. Hoa, T.T.N.; Le, D.T.T.; Van Toan, N.; Van Duy, N.; Hung, C.M.; Van Hieu, N.; Hoa, N.D. Highly selective H<sub>2</sub>S gas sensor based on WO<sub>3</sub>-coated SnO<sub>2</sub> nanowires. *Mater. Today Commun.* 2021, 26, 102094.
7. Ho, D.M.; Ho, B.Q.; Le, T.V. Evaluate of air pollution dispersion and propose planing scenerios to reduce air pollution for livestock activities in Tan Thanh district, Ba Ria—Vung Tau province. *Sci. Technol. Dev. J. Sci. Earth Environ.* 2019, 2, 26–37.
8. Asad, M.; Sheikhi, M.H.; Pourfath, M.; Moradi, M. High sensitive and selective flexible H<sub>2</sub>S gas sensors based on Cu nanoparticle decorated SWCNTs. *Sens. Actuators B Chem.* 2015, 210, 1–8.
9. Padua, L.M.G.; Yeh, J.-M.; Santiago, K.S. A Novel Application of Electroactive Polyimide Doped with Gold Nanoparticles: As a Chemiresistor Sensor for Hydrogen Sulfide Gas. *Polymers* 2019, 11, 1918.
10. Somacescu, S.; Stanoiu, A.; Dinu, I.V.; Calderon-Moreno, J.M.; Florea, O.G.; Florea, M.; Osiceanu, P.; Simion, C.E. CuWO<sub>4</sub> with CuO and Cu(OH)<sub>2</sub> native surface layers for H<sub>2</sub>S detection under in-field conditions. *Materials* 2021, 14, 465.
11. Hsu, K.-C.; Fang, T.-H.; Hsiao, Y.-J.; Li, Z.-J. Rapid detection of low concentrations of H<sub>2</sub>S using CuO-doped ZnO nanofibers. *J. Alloy. Compd.* 2021, 852, 157014.
12. Peng, F.; Sun, Y.; Lu, Y.; Yu, W.; Ge, M.; Shi, J.; Cong, R.; Hao, J.; Dai, N. Studies on Sensing Properties and Mechanism of CuO Nanoparticles to H<sub>2</sub>S Gas. *Nanomaterials* 2020, 10, 774.
13. Ali, F.I.M.; Mahmoud, S.T.; Awwad, F.; Greish, Y.E.; Abu-Hani, A.F.S. Low power consumption and fast response H<sub>2</sub>S gas sensor based on a chitosan-CuO hybrid nanocomposite thin film. *Carbohydr. Polym.* 2020, 236, 116064.
14. Hittini, W.; Abu-Hani, A.F.; Reddy, N.; Mahmoud, S.T. Cellulose-Copper Oxide hybrid nanocomposites membranes for H<sub>2</sub>S gas detection at low temperatures. *Sci. Rep.* 2020, 10, 1–9.
15. Pravarthana, N.D.; Tyagi, A.; Jagadale, T.C.; Prellier, W.; Aswal, D.K. Highly sensitive and selective H<sub>2</sub>S gas sensor based on TiO<sub>2</sub> thin films. *Appl. Surf. Sci.* 2021, 549, 149281.

16. Mokoena, T.P.; Tshabalala, Z.P.; Hillie, K.T.; Swart, H.C.; Motaung, D.E. The blue luminescence of p-type NiO nanostructured material induced by defects: H<sub>2</sub>S gas sensing characteristics at a relatively low operating temperature. *Appl. Surf. Sci.* 2020, 525, 146002.
17. Tang, Y.; Wu, W.; Wang, B.; Dai, X.; Xie, W.; Yang, Y.; Zhang, R.; Shi, X.; Zhu, H.; Luo, J.; et al. H<sub>2</sub>S gas sensing performance and mechanisms using CuO-Al<sub>2</sub>O<sub>3</sub> composite films based on both surface acoustic wave and chemire-sistor techniques. *Sens. Actuators B Chem.* 2020, 325, 128742.
18. Wu, Y.-Y.; Song, B.-Y.; Zhang, X.-F.; Deng, Z.-P.; Huo, L.-H.; Gao, S. Microtubular  $\alpha$ -Fe<sub>2</sub>O<sub>3</sub>/Fe<sub>2</sub>(MoO<sub>4</sub>)<sub>3</sub> heterostructure derived from absorbent cotton for enhanced ppb-level H<sub>2</sub>S gas-sensing performance. *J. Alloy. Compd.* 2021, 867, 158994.
19. El-Shamy, A.G. New nano-composite based on carbon dots (CDots) decorated magnesium oxide (MgO) nano-particles () sensor for high H<sub>2</sub>S gas sensitivity performance. *Sens. Actuators B Chem.* 2021, 329, 129154.
20. Yang, D.; Chen, G.; Fu, J.; Zhu, Y.; Dai, Z.; Wu, L.; Liu, J. The mitigation performance of ventilation on the accident consequences of H<sub>2</sub>S-containing natural gas release. *Process Saf. Environ. Prot.* 2021, 148, 1327–1336.
21. Yang, S.; Sun, J.; Xu, L.; Zhou, Q.; Chen, X.; Zhu, S.; Dong, B.; Lu, G.; Song, H. functionalized three-dimensional macroporous WO<sub>3</sub>: A application of selective H<sub>2</sub>S gas sensor for exhaled breath biomarker detection. *Sens. Actuators B Chem.* 2020, 324, 128725.
22. Song, B.-Y.; Zhang, M.; Teng, Y.; Zhang, X.-F.; Deng, Z.-P.; Huo, L.-H.; Gao, S. Highly selective ppb-level H<sub>2</sub>S sensor for spendable detection of exhaled biomarker and pork freshness at low temperature: Mesoporous SnO<sub>2</sub> hierarchical architectures derived from waste scallion root. *Sens. Actuators B Chem.* 2020, 307, 127662.
23. Pandey, S.K.; Kim, K.-H.; Tang, K.-T. A review of sensor-based methods for monitoring hydrogen sulfide. *TrAC Trends Anal. Chem.* 2012, 32, 87–99.
24. Vuong, N.M.; Chinh, N.D.; Huy, B.T.; Lee, Y.-I. CuO-Decorated ZnO hierarchical nanostructures as efficient and established sensing materials for H<sub>2</sub>S gas sensors. *Sci. Rep.* 2016, 6, 26736.
25. Ali, F.I.M.; Awwad, F.; Greish, Y.E.; Mahmoud, S.T. Hydrogen Sulfide (H<sub>2</sub>S) Gas Sensor: A Review. *IEEE Sens. J.* 2019, 19, 2394–2407.
26. Peng, F.; Sun, Y.; Yu, W.; Lu, Y.; Hao, J.; Cong, R.; Shi, J.; Ge, M.; Dai, N. Gas sensing performance and mechanism of CuO(p)-WO<sub>3</sub>(n) composites to H<sub>2</sub>S gas. *Nanomaterials* 2020, 10, 1162.
27. Kim, J.-Y.; Lee, J.-H.; Kim, J.-H.; Mirzaei, A.; Kim, H.W.; Kim, S.S. Realization of H<sub>2</sub>S sensing by Pd-functionalized networked CuO nanowires in self-heating mode. *Sens. Actuators B Chem.* 2019, 299, 126965.

28. Mirzaei, A.; Leonardi, S.G.; Neri, G. Detection of hazardous volatile organic compounds (VOCs) by metal oxide nanostructures-based gas sensors: A review. *Ceram. Int.* 2016, 42, 15119–15141.
29. Mirzaei, A.; Neri, G. Microwave-assisted synthesis of metal oxide nanostructures for gas sensing application: A review. *Sens. Actuators B Chem.* 2016, 237, 749–775.
30. Nasri, A.; Pétrissans, M.; Fierro, V.; Celzard, A. Gas sensing based on organic composite materials: Review of sensor types, progresses and challenges. *Mater. Sci. Semicond. Process.* 2021, 128, 105744.
31. Ayes, A.I.; Abu-Hani, A.F.; Mahmoud, S.T.; Haik, Y. Selective H<sub>2</sub>S sensor based on CuO nanoparticles embedded in organic membranes. *Sens. Actuators B Chem.* 2016, 231, 593–600.
32. Boepple, M.; Zhu, Z.; Hu, X.; Weimar, U.; Barsan, N. Impact of heterostructures on hydrogen sulfide sensing: Example of core-shell CuO/CuFe<sub>2</sub>O<sub>4</sub> nanostructures. *Sens. Actuators B Chem.* 2020, 321, 128523.
33. Nadargi, D.Y.; Tamboli, M.S.; Patil, S.S.; Dateer, R.B.; Mulla, I.S.; Choi, H.; Suryavanshi, S.S. Microwave-Epoxy-Assisted Hydrothermal Synthesis of the CuO/ZnO Heterojunction: A Highly Versatile Route to Develop H<sub>2</sub>S Gas Sensors. *ACS Omega* 2020, 5, 8587–8595.
34. Paul, A.; Weinberger, C.; Tiemann, M.; Wagner, T. Copper Oxide/Silica Nanocomposites for Selective and Stable H<sub>2</sub>S Gas Detection. *ACS Appl. Nano Mater.* 2019, 2, 3335–3338.
35. Balsamo, M.; Cimino, S.; de Falco, G.; Erto, A.; Lisi, L. ZnO-CuO supported on activated carbon for H<sub>2</sub>S removal at room temperature. *Chem. Eng. J.* 2016, 304, 399–407.
36. Van Toan, N.; Hung, C.M.; Hoa, N.D.; Van Duy, N.; Le, D.T.T.; Viet, N.N.; Phuoc, P.H.; Van Hieu, N. Enhanced NH<sub>3</sub> and H<sub>2</sub> gas sensing with H<sub>2</sub>S gas interference using multilayer SnO<sub>2</sub>/Pt/WO<sub>3</sub> nanofilms. *J. Hazard. Mater.* 2021, 412, 125181.
37. Hu, Q.; Zhang, W.; Wang, X.; Wang, Q.; Huang, B.; Li, Y.; Hua, X.; Liu, G.; Li, B.; Zhou, J.; et al. Binder-free CuO nanoneedle arrays based tube-type sensor for H<sub>2</sub>S gas sensing. *Sens. Actuators B Chem.* 2021, 326, 128993.
38. Huang, Z.; Wang, X.; Sun, F.; Fan, C.; Sun, Y.; Jia, F.; Yin, G.; Zhou, T.; Liu, B. Super response and selectivity to H<sub>2</sub>S at room temperature based on CuO nanomaterials prepared by seed-induced hydrothermal growth. *Mater. Des.* 2021, 201, 109507.
39. Miao, J.; Chen, C.; Lin, J.Y. Humidity independent hydrogen sulfide sensing response achieved with monolayer film of CuO nanosheets. *Sens. Actuators B Chem.* 2020, 309, 127785.
40. Dhakshinamoorthy, J.; Pullithadathil, B. New Insights Towards Electron Transport Mechanism of Highly Efficient p-Type CuO (111) Nanocuboids-Based H<sub>2</sub>S Gas Sensor. *J. Phys. Chem. C* 2016, 120, 4087–4096.

41. Zhang, F.; Zhu, A.; Luo, Y.; Tian, Y.; Yang, J.; Qin, Y. CuO Nanosheets for Sensitive and Selective Determination of H<sub>2</sub>S with High Recovery Ability. *J. Phys. Chem. C* 2010, 114, 19214–19219.
42. Li, X.; Wang, Y.; Lei, Y.; Gu, Z. Highly sensitive H<sub>2</sub>S sensor based on template-synthesized CuO nanowires. *RSC Adv.* 2012, 2, 2302–2307.
43. Hosseini, Z.S.; Mortezaali, A.; Iraj, A.; Fardindoost, S. Sensitive and selective room temperature H<sub>2</sub>S gas sensor based on Au sensitized vertical ZnO nanorods with flower-like structures. *J. Alloy. Compd.* 2015, 628, 222–229.
44. Zhou, Q.; Xu, L.; Umar, A.; Chen, W.; Kumar, R. Pt nanoparticles decorated SnO<sub>2</sub> nanoneedles for efficient CO gas sensing applications. *Sens. Actuators B Chem.* 2018, 256, 656–664.
45. Ngoc, T.M.; Van Duy, N.; Hung, C.M.; Hoa, N.D.; Nguyen, H.; Tonezzer, M.; Van Hieu, N. Self-heated Ag-decorated SnO<sub>2</sub> nanowires with low power consumption used as a predictive virtual multisensor for H<sub>2</sub>S-selective sensing. *Anal. Chim. Acta* 2019, 1069, 108–116.
46. Sarıca, N.; Alev, O.; Arslan, L.Ç.; Öztürk, Z.Z. Characterization and gas sensing performances of noble metals decorated CuO nanorods. *Thin Solid Films* 2019, 685, 321–328.
47. Rydosz, A.; Maziarz, W.; Pisarkiewicz, T.; Wincza, K.; Gruszczyński, S. Nano-thin CuO films doped with Au and Pd for gas sensors applications. In *Proceedings of the International Conference on Informatics, Electronics & Vision, Dhaka, Bangladesh, 17–18 May 2013*; pp. 1–5.
48. Kim, H.; Jin, C.; Park, S.; Kim, S.; Lee, C. H<sub>2</sub>S gas sensing properties of bare and Pd-functionalized CuO nanorods. *Sens. Actuators B Chem.* 2012, 161, 594–599.
49. Mikami, K.; Kido, Y.; Akaishi, Y.; Quitain, A.; Kida, T. Synthesis of Cu<sub>2</sub>O/CuO nanocrystals and their application to H<sub>2</sub>S sensing. *Sensors* 2019, 19, 211.
50. Hu, X.; Zhu, Z.; Chen, C.; Wen, T.; Zhao, X.; Xie, L. Highly sensitive H<sub>2</sub>S gas sensors based on Pd-doped CuO nanoflowers with low operating temperature. *Sens. Actuators B Chem.* 2017, 253, 809–817.

---

Retrieved from <https://encyclopedia.pub/entry/history/show/26504>